Front. Phys., 2012, 7(6): 714–720
DOI 10.1007/s11467-012-0267-7

RESEARCH ARTICLE

Study on parameters influencing analytical performance of laser-induced breakdown spectroscopy

Yong Zhang*, **Yun-Hai Jia**†, **Jin-Wen Chen**, **Xue-Jing Shen**, **Lei Zhao**, **Chun Yang**, **Yong-Yan Chen**, **Yong-Hui Zhang**, **Peng-Cheng Han**

National Analysis Center for Iron and Steel, Central Iron & Steel Research Institute, Beijing 100081, China

*E-mail: *chauchylan@163.com, †jyh@analysis.org.cn*

Received May 27, 2012; accepted September 4, 2012

Lens-to-sample distances, delay time, atmospheric condition, laser pulse energy, etc. had obvious effects on the analytical performance of laser-induced breakdown spectroscopy. In this paper, these parameters are investigated in greater detail and we will explain how they have influences on the analytical performance. The results show that the focal plane under the sample surface can improve precision and detection limit, and the delay time should be decided according to sensitivity and accuracy. Spectral line intensity is stronger in argon than helium, nitrogen and air gas environment. Pulse energy should exceed energy threshold (about 50 mJ) which can generate plasma, and the energy should not exceed about 300 mJ to avoid plasma shielding. Under optimum parameters, concentration relative standard deviation of C, Si, Mn, P, S, Ni, and Cr for low-alloyed steel (sample number 11278) which were measured 11 times is 2.37%, 2.18%, 2.23%, 7.8%, 9.34%, 1.92%, and 2.13%, respectively. And the detection limit of C, Si, Mn, P, S, Ni, and Cr for pure steel is 0.0045%, 0.0072%, 0.0069%, 0.0027%, 0.0024%, 0.0047%, and 0.0024%, respectively.

Keywords laser-induced breakdown spectroscopy (LIBS), analytical performance, plasma diagnosis, plasma shielding

PACS numbers 52.25.Kn, 52.25.Os

1 Introduction

Since 1960 when the first ruby laser system was born, laser technology has put new vigor to analytical chemistry, such as laser Raman, LA-ICP-MS/OES, laser-induced mass spectroscopy (LIMS), laser-induced fluorescence spectroscopy (LIFS), and laser-induced breakdown spectroscopy (LIBS). Particularly, the advantage of laser-induced breakdown spectroscopy is no or little need for sample preparation, simple apparatus, remote and online analysis, less sample consumption, so in the field of inorganic element analysis, it caused extensive concern of analytical chemists. At present, research of LIBS is focused on diagnosis of plasma [1, 2], bulk analysis [3, 4] and microanalysis [5, 6], dual or multiple pulse to improve analytical sensitivity [7, 8], calibration free analysis [9, 10] and chemometrics combined with LIBS to correct matrix effect [11, 12], etc. Among them, research on plasma diagnosis is very important, because it is the foundation of bulk analysis and microanalysis.

Several researchers have investigated on this subject. Aguilera studied laser ablation of steel in air at atmospheric pressure for varying pulse energies and focusing distances, these parameters strongly influence the analytical performance of LIBS. They used CCD as the detector [13]. Dimtro established that pulse energy absorption in the plasma plume decreases when the sample is inclined with respect to the laser radiation direction, and it will improve analytical sensitivity [14]. They used photocell as the detector. In this paper, the influence of spectral line intensity, such as lens-to-sample distance, delay time, background gas and pressure, pulse energy and so on, are investigated in detail by photomultiplier tube (PMT), which can record spectral line intensity variation according to pulse numbers along depth direction.

2 Instrumental setup and test sample

Q-switch Nd:YAG laser (continuum surelite III, wavelength 1064 nm, pulse width 5.3 ns, pulse to pulse energy stability 2.5%, pulse frequency 10 Hz, pulse energy from 0 to 910 mJ, nearly Gaussian distribution, beam waist diameter 9 mm) consists of a sample chamber which can be filled with argon, stepping motors which can drive sample stage to move along x, y, and z axis. Paschen–Runge spectrometer (focal length 750 mm, photomultiplier tube), pulse delay generator and etc. The focal length of lens is 100 mm to focus laser beam. When plasma is generated, there is a convex lens to collect photon coming from plasma and the compound light is dispersed by concave grating. There is a gas flow meter to control gas flow rate and a barometer to display pressure of the sample chamber, and the experimental setup is shown in Fig. 1.

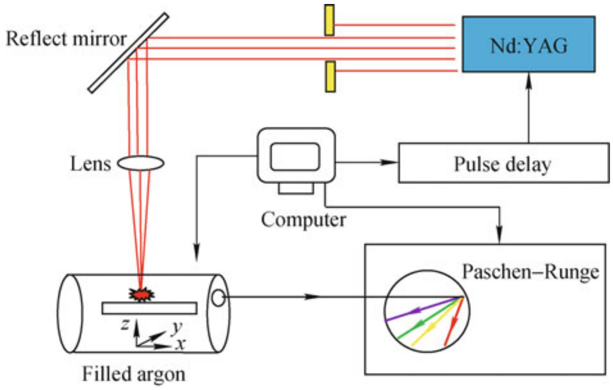

Fig. 1 Schematic setup of LIBS.

The sample number of S9259 (GSBH 40078-94, carbon steel) is investigated; the sample is ground by ground machine for spectra analysis. The mesh number of particle size for sand paper is 40. The mass fraction of C, Si, Mn, P, S, Cr, and Ni for S9259 is 1.23%, 0.805%, 1.78%, 0.093%, 0.032%, 0.321%, and 0.445%, respectively. For the sample number 11278 (low alloy steel), the mass fraction of C, Si, Mn, P, S, Cr, and Ni is 0.427%, 1.13%, 0.800%, 0.021%, 0.020%, 1.07%, and 0.414%, respectively.

3 Influence of spectra line intensity under different experimental conditions

3.1 Influence of spectra line intensity on varying lens-to-sample distances

3.1.1 Determination of focal point position and laser ablation morphology

Focal point position can be determined based on that the spot of laser ablation is the minimum and the depth is the deepest in the vicinity of the focal point. Laser ablation morphology for the sample number of S9259 is shown in Fig. 2 for varying lens-to-sample distances.

The meaning of labels in Fig. 2 is the scale of lens position. It can be seen from Fig. 2 that the minimum and deepest spot corresponds to the position of 22 mm (depth is about 91 μm, measured by laser confocal microscope), so the focal point corresponds to 22 mm. When the focal plane is inside the sample (such as position of

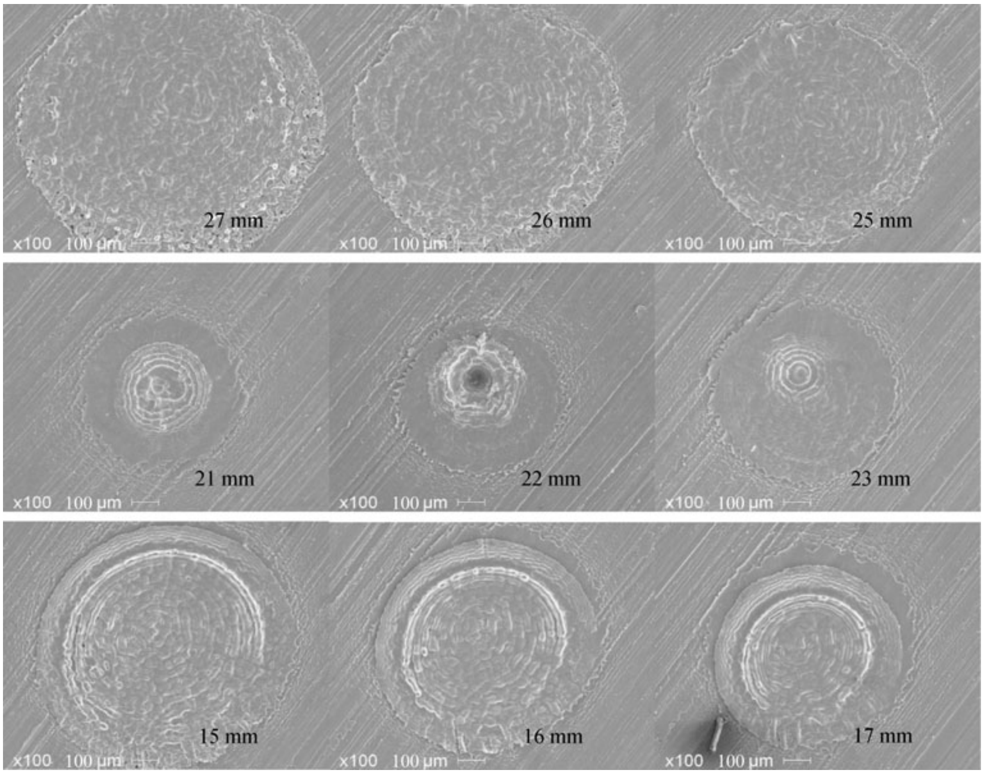

Fig. 2 SEM surface topography of laser ablation for Fe matrix (pulse energy 296 mJ, 60 pulses, argon pressure about 4000 Pa, flow rate 1.8 L/min. Label numbers is the scale of lens position).

15 mm, 16 mm, 17 mm), the ablation spot diameter is larger than the lens focal plane position in the vicinity of sample surface. The nearer from lens-to-sample distances, the larger the ablation spot diameter is (depth is about 55 μm corresponding to 15 mm). Meanwhile, there is deposit matter on the edge of ablation crater obviously; this is cooling plasma deposit on the edge of ablation crater. When the lens focal plane position is above the sample surface (such as position of 25 mm, 26 mm, 27 mm), the ablation crater is larger and shallower than the focal plane position inside the sample, the farther from lens-to-sample distances, the larger and shallower the crater is (depth is about 32 μm corresponding to 27 mm).

3.1.2 Influence of spectra line intensity for varying lens-to-sample distances

The lens position is set to zero (scale position 22 mm) when the lens focal plane is coincident with the sample surface. The number is a positive sign when the lens focal plane is inside the sample; conversely, the number is a negative sign corresponding to the focal plane above the sample surface. The spectra line intensity of C, Si, Mn, P, S, Cr, Ni, and Fe elements for steel sample (GSBH S9259) having changed by varying lens-to-sample distances is shown in Fig. 4.

Figure 4 is very similar to Fig. 7 of reference, which uses double pulses [15]. It can be seen that starting from the nearest position of lens-to-sample distances, with the distance increasing, the characteristic line intensity is more and more stronger. In the vicinity of 4 mm position, the line intensity reaches the maximum, then it decreases. In the vicinity of the focal point, the line intensity changes greatly and quickly, and the line intensity is not too high. This is possibly because in the vicinity of the focal point, the irradiance is very high and produces a plasma shielding effect [16], which leads the plasma to interact with the laser, and a portion of the pulse energy is absorbed by the plasma. Another reason is likely

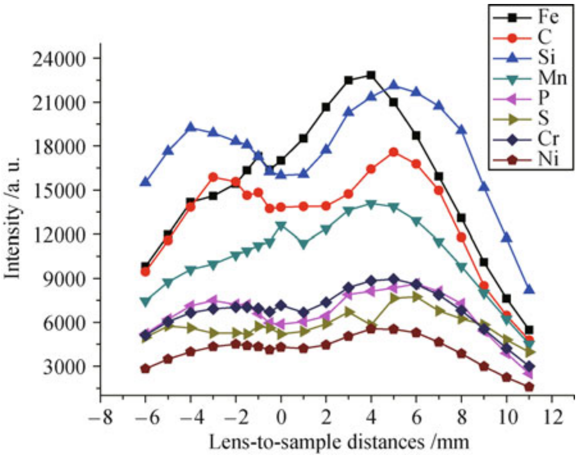

Fig. 4 Spectra line intensity influenced by different lens-to-sample distances.

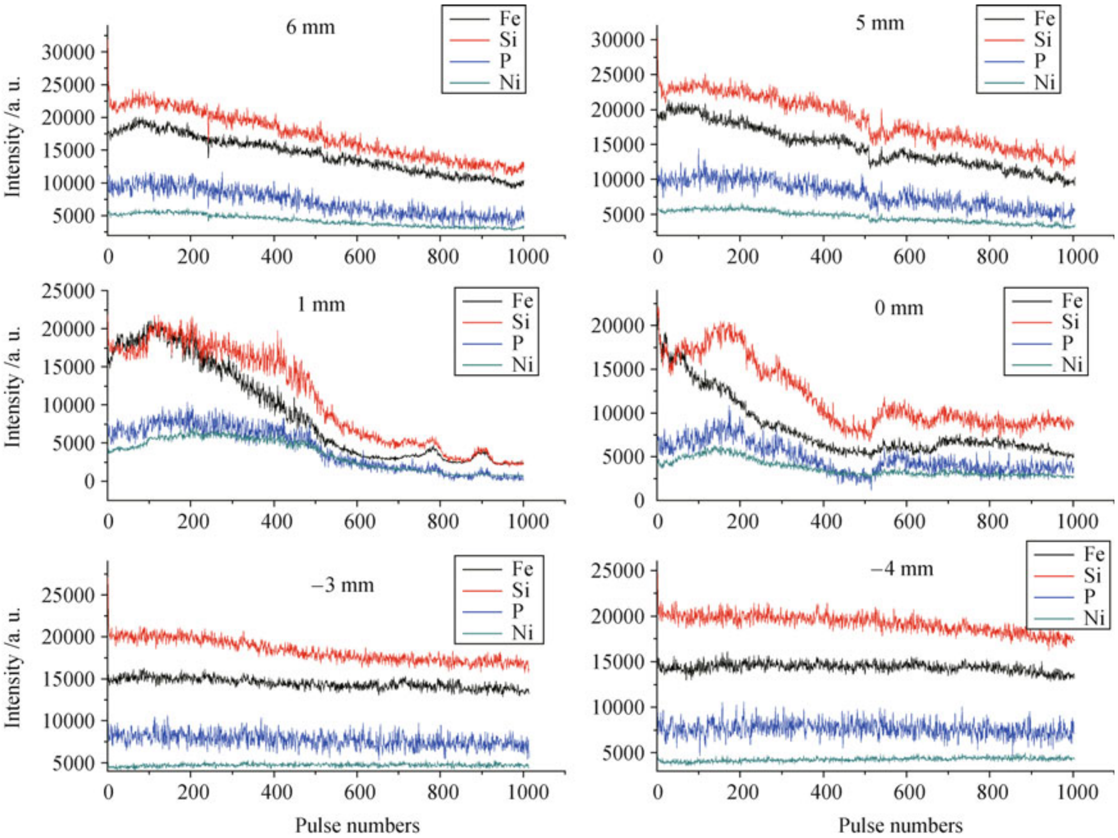

Fig. 5 Spectra line intensity variation according to pulse numbers at different focal plane positions.

that with the depth being deeper and deeper, the pulse energy coupling with the matter is getting smaller and smaller, so the spectral line intensity changes greatly and quickly. When the lens focal plane is above the sample surface, with the distance increasing, the characteristic line intensity is getting weaker and weaker, which is because the laser ablation crater diameter is getting larger, then the irradiance gets smaller and the line intensity is decreasing slowly. Compared with the lens focal plane inside the sample, the line intensity changes quite slower because the depth of the laser ablation crater is much shallower, and the laser ablation rate is almost homogeneous. The spectra line intensity variation at different lens-to-sample (1000 pulses) positions is shown in Fig. 5.

It can be seen from Fig. 5 that, when the lens focal plane is above the sample surface (−3 mm, −4 mm), the spectra line intensity variation is very small; in the vicinity of the focal point the spectra line intensity decreases quickly; and when the lens focal plane is inside the sample (5 mm, 6 mm), the spectra line intensity changes slowly first, and with the laser ablation depth getting deeper, the spectra line intensity decreases slowly. In general, in order to avoid gas breakdown, the focal plane should be kept inside the sample.

3.2 Delay time

LIBS belongs to the pulse plasma source. In general, at early times, free-free transition (Bremsstrahlung) and free-bound transition (recombination) result in strong background continuum which decays with time more quickly than characteristic spectral line [17]. The delay from the initiation of the laser to the opening of the window is named delay time. The sample chamber is filled with argon, and pressure 4000 Pa, flow rate 1.8 L/min, pulse energy 296 mJ, focal plane above sample surface 4 mm, integration time 100 μs. The spectral line intensity of Fe, C, Si, Mn, P, S, Cr, and Ni etc. for steel sample (sample number S9259) varied according to different delay time is shown in Fig. 6.

It can be seen from Fig. 6 that, with delay time increasing, the spectra line intensity is decreasing, which is because with the time evolution, the electron number density and excitation temperature in the plasma is decreasing, so the spectra line intensity is decreasing, too. The delay time should not be too long. If too long, the analytical sensitivity will be too low and trace elements cannot be detected; meanwhile, the delay time should not be too short. Otherwise, the background continuum will be too strong, which will affect the analytical accuracy. Given this experimental condition, the life of plasma is about 25 μs.

3.3 Influence of spectra line intensity on varying pulse energy

Pulse energy has a great influence on spectra line intensity. The focal plane is above the sample surface by 4 mm, the sample chamber is filled with argon and the pressure is maintained about 4000 Pa. (If the focal plane is above the sample surface, there is always a danger of gas breakdown, but if the gas pressure is kept very low, even argon breakdown, the plasma absorbs a small portion of the pulse energy. In argon environment, the pressure is maintained about 4000 Pa, the flow rate is 1.8 L/min, and the spectral line intensity for all elements reaches maximum) The spectral line intensity of Fe, Si, Mn, P, S, Cr, and Ni for steel sample (GSBH S9259) is shown in Fig. 7.

It can be seen from Fig. 7 that, the pulse energy is too low (lower than 50 mJ), and the spectral line intensity is close to the background intensity. It means that the pulse energy should be greater than the threshold [18]. With the pulse energy increasing, the spectral line intensity is increasing, too, which is because the irradiance is increasing with the increase of the pulse energy. The spectral line intensity is saturated when the pulse energy is too high (more than 300 mJ). One reason might be that it will result in a plasma shielding effect: A portion of the pulse energy is absorbed by the plasma. Another reason might be the self-absorption, due to which

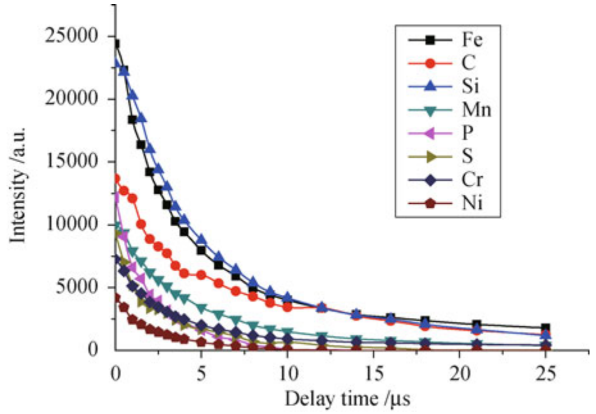

Fig. 6 Spectral line intensity variation according to delay time.

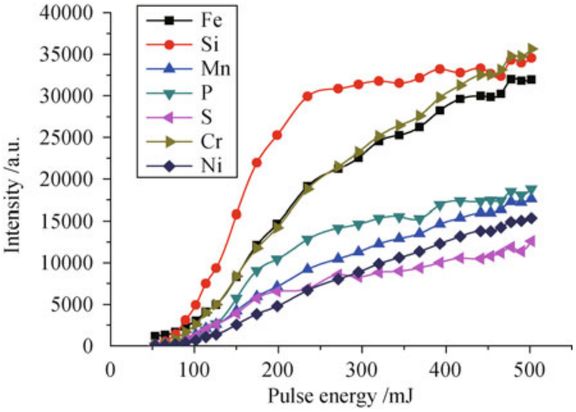

Fig. 7 Relationship between pulse energy and spectral line intensity.

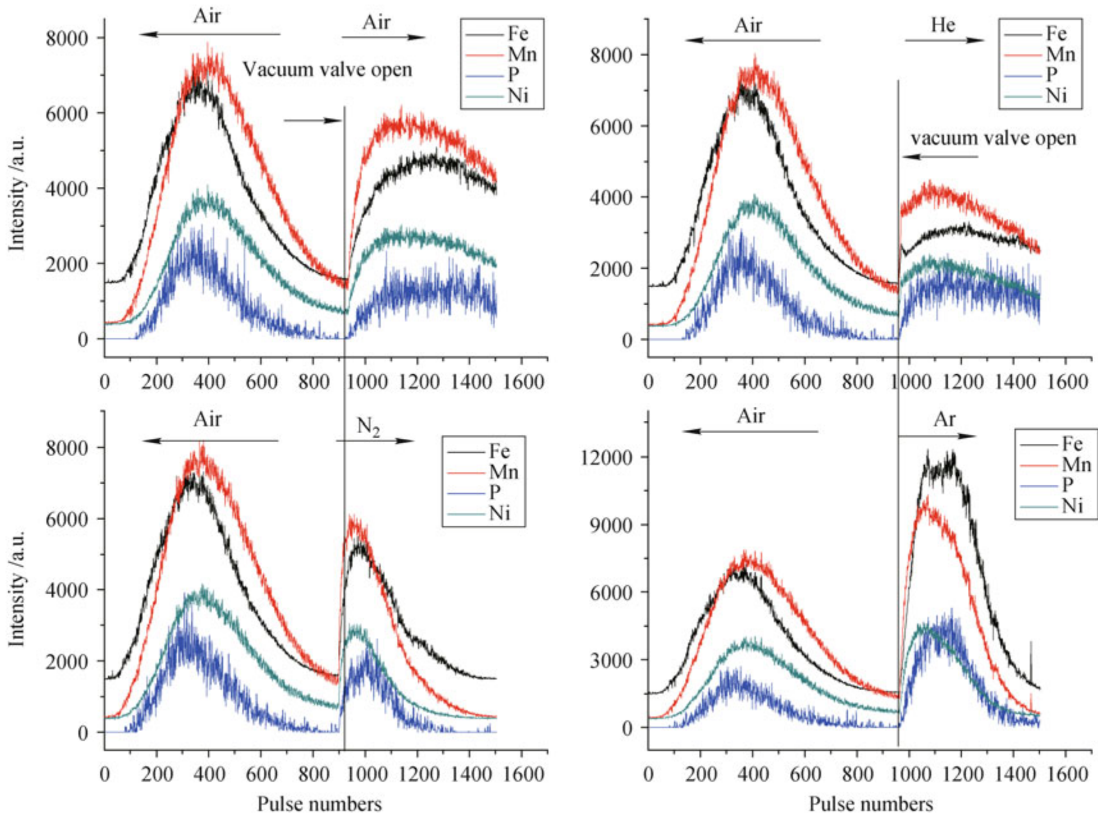

Fig. 8 Effect of different gases and pressures.

the spectral line intensity is increasing very slowly.

3.4 Effects of surrounding gas on spectral line intensity

Spectra line intensity is influenced by surrounding gas and its pressure. Many research papers have been published on this topic [19–22]. The focal plane is above the sample surface by 4 mm, with the pulse energy 296 mJ. The sample number GSBH S9259 is placed into a chamber, and pumped from atmosphere pressure to 220 Pa by mechanical pump and the vacuum valve is open. The surrounding gas is filled into the sample chamber. Meanwhile, the laser is firing ceaselessly. The spectral line intensity of Fe, Mn, P, Ni is shown in Fig. 8.

The arrows indicate that the pressure is increasing. The first peak is produced in air from atmosphere pressure to 220 Pa, and the second peak is produced in different gases from 220 Pa to atmosphere pressure. It can be seen from Fig. 8 that the sensitivity is different in different surrounding gas. The order of sensitivity is Ar > Air > N_2 > He. The sensitivity in argon is higher than that in helium because the ionization energy of argon is less than helium (argon ionization energy 15.76 eV, helium ionization energy 24.59 eV), so argon is easily ionized than helium and produces many electrons which result in cascade collision with ion and neutral atom. Besides, the thermal conductivity coefficient of argon is less than helium, which results in that the speed of thermal diffusion in argon is lower than in helium, so the life of plasma in argon is longer than helium. The ionization energy of argon is similar with oxygen and nitrogen, but the spectral line intensity in oxygen and nitrogen is less than in argon. It is because the thermal conductivity coefficient of oxygen and nitrogen is higher than argon, which causes that the speed of thermal diffusion in oxygen and nitrogen is faster than in argon, and the plasma life in oxygen and nitrogen is less than in argon. In addition, in atmosphere environment, the temperature of plasma is so high that the analyte is combined with the oxygen atom, and the number of excited atoms is fewer than in argon, so the spectral line intensity is weaker than in argon.

From Fig. 8, it can be seen that in argon, air, nitrogen, helium environment, with the pressure increasing, the spectral line intensity is increasing, too. When the pressure reaches a certain level, the spectral line intensity is decreasing. The reason is that, at low pressure, the electron number density in plasma is very few, the excitation temperature is too low, and the amount of excited atoms is few, so the spectral line intensity is weaker. Besides, at low pressure, plasma cannot be confined in a small space; it escapes much faster, and the heat energy gets lost quickly. With the pressure increasing, the electron number density and excitation temperature is increasing in plasma. In addition, the plasma is confined in a small space, not easy to escape, so the plasma life is longer than in low pressure. When the pressure is too high, with the pressure increasing, the spectral line intensity is decreasing. This is because there are many electrons and ions which interact with the laser in plasma, which results in that many photons cannot reach the sample surface, so the spectral line intensity is weaker. The pulse energy absorbed by plasma can be described by the following equation [23]:

$$k_{\mathrm{IB}} = \left[1 - \exp\left(-\frac{hc}{\lambda cT}\right)\right] \frac{4e^6\lambda^3}{3hc^4 m_e} \cdot \left(\frac{2\pi}{3m_e kT}\right)^{1/2} n_e \sum_i z_i^2 n_i g_i \qquad (1)$$

z_i, n_e, g_i represent charge number, electron number density and Gaunt correct factor, respectively. From the above formula, we can see that the bigger the electron number density and charge number, the more intense the interaction of laser with plasma is, and so few photons reach the sample surface.

The focal plane is inside the sample by 5 mm. The sample chamber is filled with argon, flow rate 1.8 L/min, pressure maintained about 4000 Pa, output energy kept about 300 mJ per pulse. The spectral line wavelength, delay time, integration time and spectra line order for specific elements are shown in Table 1.

Table 1 Delay time, integration time, and wavelength for specific elements.

Elements	Spectra line order	Wavelength /nm	Delay time /μs	Integration time /μs
C	1	193.1	1.5	100
Si	1	212.4	1	100
Mn	1	293.3	1	100
P	1	178.3	1.5	100
S	1	180.7	1.5	100
Cr	1	267.7	0.5	100
Ni	1	215.8	0.5	100
Fe	1	273.0	1.5	100

Under this optimum parameters, concentration relative standard deviation for the sample number 11278, which is measured 11 times, and the detection limits (determined by pure steel sample, $LOD = 3\sigma/\mathrm{S}$) for C, Si, Mn, P, S, Cr, and Ni are shown in Table 2.

Table 2 Relative standard deviation and detection limit for LIBS.

	C	Si	Mn	P	S	Ni	Cr
Relative standard deviation	2.37	2.18	2.23	5.12	9.34	1.92	2.13
Detection limits	0.0045	0.0072	0.0069	0.0027	0.0024	0.0047	0.0024

Note: All data are in %. C, Si, Mn, P, S, Cr, Ni (spectroscopic standard CRM number ss401/2 ∼ ss410/2, produced by BAS) is analyzed by LIBS-OPA 100 and Laboratory Spark 750, Results provided by LIBS agree with Spark-OES.

4 Conclusion

From the above analysis, we can see that the lens-to-sample distance, delay time, atmosphere condition and pulse energy have great influences on the spectra line intensity. The lens-to-sample distance should be decided by analytical target. The focal plane should be above the sample surface when the depth profile analysis is carried on, which can improve the depth analysis resolution. Analytical sensitivity can be improved when the focal plane is put inside the sample. Delay time can be chosen according to the sensitivity and accuracy. In different atmosphere conditions, the strongest sensitivity is produced in argon under optimum parameters. Analytical performance such as precision, accuracy and detection limit for LIBS is improved significantly.

Acknowledgements This work was supported by the Special Fund of National Important Instrument (Grant No. 2011YQ140147), and we would like to thank Prof. Jin Yu for helpful discussion.

References

1. V. Bulatov, L. Xu, and I. Schechter, Anal. Chem., 1996, 68(17): 2966
2. J. A. Aguilera and C. Aragón, Spectrochim. Acta B, 2004, 59: 1861
3. R. Noll, H. Bette, A. Brysch, M. Kraushaar, I. Monch, L. Peter, and V. Sturm, Spectrochim. Acta B, 2001, 56: 637
4. M. Hemmerlin, R. Meilland, H. Falk, P. Wintjens, and L. Paulard, Spectrochim. Acta B, 2001, 56: 661
5. H. Bette, R. Noll, G. Müller, H. W. Jansen, Ç. Nazikkol, and H. Mittelstädt, J. Laser Appl., 2005, 17(3): 183
6. H. M. Kuss, H. Mittelstaedt, and G. Mueller, J. Anal. At. Spectrom., 2005, 20(8): 730
7. R. Sattmann, V. Sturm, and R. Noll, J. Phys. D, 1995, 28(10): 2181
8. F. Colao, V. Lazic, R. Fantoni, and S. Pershin, Spectrochim. Acta B, 2002, 57: 1167
9. A. Ciucci, M. Corsi, V. Palleschi, S. Rastelli, A. Salvetti, and E. Tognoni, Appl. Spectrosc., 1999, 53(8): 960
10. E. Tognoni, G. Cristoforetti, S. Legnaioli, and V. Palleschi, Spectrochim. Acta B, 2010, 65: 1
11. Z. Wang, F. Jie, L. Z. Li, W. D. Ni, and Z. Li, J. Anal. At. Spectrom., 2011, 26(11): 2289
12. J. B. Sirven, B. Bousquet, L. Canioni, and L. Sarger, Anal. Chem., 2006, 78(5): 1462
13. J. A. Aguilera, C. Aragón, and F. A. Peñalba, Appl. Surf. Sci., 1998, 127–129: 309

14. G. Dimitro and T. Zheleva, Spectrochim. Acta B, 1984, 39: 1209
15. R. Sattmann, V. Sturm, and R. Noll, J. Phys. D, 1995, 28(10): 2181
16. E. H. Piepmeier and H. V. Malmstadt, Anal. Chem., 1969, 41(6): 700
17. R. Wisbrun, I. Schechter, R. Niessner, H. Schroeder, and K. L. Kompa, Anal. Chem., 1994, 66(18): 2964
18. L. M. Cabalín and J. J. Laserna, Spectrochim. Acta B, 1998, 53: 723
19. Y. Iida, Spectrochim. Acta B, 1990, 45: 1353
20. A. W. Effenberger and J. R. Scott, Sensors, 2010, 10(5): 4907
21. C. B. Dreyer, G. S. Mungas, P. Thanh, and J. G. Radziszewski, Spectrochim. Acta B., 2007, 62: 1448
22. L. Peter and R. Noll, Appl. Phys. B, 2007, 86(1): 159
23. L. J. Radziemski and D. A. Cremers, Laser-Induced Plasma and Applications, New York: Marcel Dekker, 1989